Journal of Sound and Vibration (1998) **209**(4), 651–669

VIBRATION OF ARBITRARILY ORIENTED TWO-MEMBER OPEN FRAMES WITH TIP MASS

D. C. D. Oguamanam and J. S. Hansen

Institute for Aerospace Studies, University of Toronto, 4925 Dufferin Street, Downsview, Ontario M3H 5T6, Canada

AND

G. R. Heppler

Systems Design Engineering, University of Waterloo, Waterloo, Ontario, N2L 3G1, Canada

(*Received* 10 *February* 1997, *and in final form* 28 *July* 1997)

A generalized two-member open frame structure is modelled using Euler–Bernoulli beam theory. The generalization is approached in two ways: an arbitrary angle between the beams; and the attachment of a payload at the end of the second beam. The linearized equations of motion are derived using Hamilton's principle and the general frequency equation, mode shapes and orthogonality condition are presented along with some numerical examples.

1. INTRODUCTION

There has been extensive research into the vibration of frame structures in many different configurations and complexities. The majority of this work has been in the area of what may be described as closed frames; the portal frame, which has three beam members, being one of the simplest examples of a closed frame. Here we use *closed frames* as an analogy for closed chains. Whereas chains of elastic bodies have joints, frames do not. Frames are chains of elastic bodies that have a fixed orientation with respect to one another. The use of *closed* has the same implication in both situations.

Some representative examples of vibration analysis of portal frames include the Rayleigh–Ritz treatment of a portal frame under support conditions that range from clamped or pinned [1, 2] to elastically supported. The latter is due to Filipich *et al*. [3], in the case of symmetric vibrations, and to Laura and Valerga De Greco [4], in the case of antisymmetric vibrations. These cases have also been treated using a more general analytical approach by Filipich and Laura [5]. Portal frames with cross-bracing and including axial deformation in the members have been treated by Chang *et al*. [6], and Mottershead *et al*. [7] have reported on the experimental identification of portal frame dynamics. More recently, Lee and Ng [8] have used the Rayleigh–Ritz method to treat portal frames, H-frames and T-frames.

Clough and Penzien [9] include a two-member closed frame as an example. It consists of two beams joined at right angles, with the end of one of them clamped and the end of the other simply supported. This example has been extended by Alexandropoulos *et al*. [10], who analyzed the free vibration of a closed two-bar frame carrying a concentrated

0022–460X/98/040651 + 19 $25.00/0/sv971251

mass with rotational inertia at its joint and including longitudinal motion as well as transverse motion of the bars.

It is relatively easy to find examples of structures that may be considered to be open frames; i.e., chains of beams that have one end fixed and the other end free. We will restrict our attention to the case of a two-member open frame which is comprised of a cantilever beam with a second beam attached to its free end. We will refer to these two-part structures with the qualifying adjective ''inclined'', the angle of inclination being measured from the undeformed axis of the beam which has the fixed end (the *first* beam) to the undeformed axis of the beam with the free end (i.e., the *second* or *distal* beam) (Figure 1). In general, the second beam may be inclined at some arbitrary angle from the axis of the first beam. One set of examples of such configurations is two-link mechanisms, such as some robots or earth moving equipment, with the joints locked [11] or, in an approximate sense, with the joints slowly moving.

When the two beams are oriented at right angles to one another, the configuration is referred to as an L-shaped structure. As an example of this kind of configuration, we note the Spacecraft Control Laboratory Experiment (SCOLE) which was modelled using the L-shaped (i.e., 90° inclination) arrangement [12].

An analytical derivation of the eigenvalues of an L-shaped structure has been presented by Bang [13], who also presents a discourse on the advantages and disadvantages of analytical solutions versus finite-dimensional approximations. It suffices to mention that the analytical approach is often more difficult to obtain and use than the finite-dimensional approximations, but it exhibits higher accuracy for simple structures. While many analysts will argue that a structure as simple as the one we are concerned with here can be more easily and just as accurately modelled using the finite element method (FEM), we hold the view that there can be circumstances in which the FEM hammer is an inappropriate tool. We will present some FEM results below that required solving a linear algebraic eigenvalue problem with 60 degrees of freedom to obtain accurate values for the first five natural frequencies. If this model were to be used as an element in a control system, it would be quickly found that having to deal with a 120 entry state vector would severely hamper the controller, and would necessitate the use of some form of model order reduction algorithm that would inevitably result in the loss of some modelling fidelity. This may or may not be acceptable, depending on the application, but with the exact eigenfunctions and natural frequencies available it would be possible to use a basis that spanned a true solution subspace without approximation; thus allowing the use of lower order models with

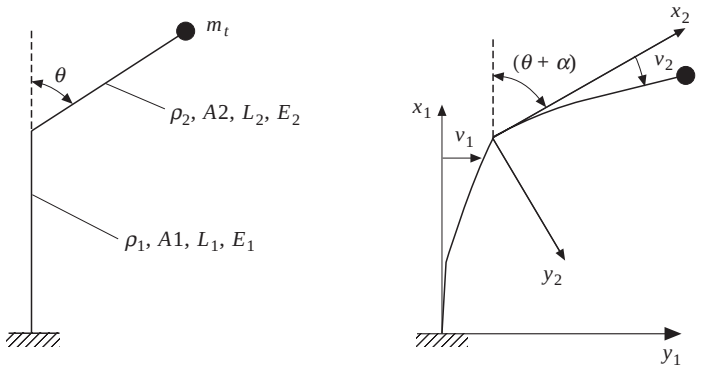

Figure 1. (a) Undeformed and (b) deformed schematics of the system.

comparable fidelity and which capture the dynamic couplings (or lack thereof) precisely. At the very least, the analytical solution offers a means of confirming the FEM model and code.

The L-shaped geometry is restrictive because design and/or operational considerations may suggest an optimal inclination which is different from 90°.

The focus of this paper is on more general planar two-beam open frame structures with an arbitrary angle of inclination between the beams and with a payload at the free tip. The aim is to present analytical expressions for the frequency equation, mode shapes and orthogonality condition for this class of frames. In our presentation, we assume that the beams are adequately modelled using a linear elastic small deformation small strain Euler–Bernoulli theory; and we derive a linearized set of governing equations of motion via Hamilton's principle, and also present the boundary conditions and the frequency equation.

2. DESCRIPTION OF THE SYSTEM

The system is composed of two flexible beam members and a payload, which are arranged as shown in Figure 1. The first beam is vertical, while the second beam is attached to the tip of the first beam such that it is inclined from the vertical by angle θ. The payload is attached at the end of the second beam and the motion of the system is assumed to be planar.

3. EQUATIONS OF MOTION

A global reference frame is attached at the base of the structure and a non-inertial frame is attached at the joint, as depicted in Figure 1. The unit vectors along the x_1 -, y_1 - and z_1 -axes of the fixed inertial frame $\mathscr{F}_a$ are, respectively, defined as $\mathbf{a}_1$, $\mathbf{a}_2$ and $\mathbf{a}_3$. Similarly, the unit vectors of the body fixed frame $\mathscr{F}_b$ are $\mathbf{b}_1$, $\mathbf{b}_2$ and $\mathbf{b}_3$, and they correspond to the x_2-, y_2- and z_2- axes of the non-inertial frame $\mathscr{F}_b$ which has its origin at the junction of the two beam segments.

The position vectors $\mathbf{r}_1$ and $\mathbf{r}_2$, measured from the base of the structure, of elemental masses of the first and second beams, respectively, are given as

$$\mathbf{r}_1(x_1, t) = x_1\,\mathbf{a}_1 + v_1(x_1, t)\mathbf{a}_2 \tag{1}$$

and

$$\mathbf{r}_2(x_2, t) = \mathbf{r}_1(L_1, t) + x_2\,\mathbf{b}_1 + v_2(x_2, t)\mathbf{b}_2, \tag{2}$$

where v_i is the transverse deflection of the ith beam.

The rotational transformation from the inertial frame to the body fixed frame is given by

$$C_{ba} = \begin{bmatrix} \cos(\theta+\alpha) & \sin(\theta+\alpha) \\ -\sin(\theta+\alpha) & \cos(\theta+\alpha) \end{bmatrix}$$

and thus equation (2) can be rewritten as

$$\mathbf{r}_2(x_2, t) = [\mathbf{a}_1 \quad \mathbf{a}_2] \begin{bmatrix} L_1 & \cos(\theta+\alpha) & -\sin(\theta+\alpha) \\ v_1(L_1, t) & \sin(\theta+\alpha) & \cos(\theta+\alpha) \end{bmatrix} \begin{Bmatrix} 1 \\ x_2 \\ v_2 \end{Bmatrix}, \tag{3}$$

where

$$\alpha(t) = \left.\frac{\partial v_1}{\partial x_1}\right|_{x_1 = L_1} \tag{4}$$

is the slope of the first beam evaluated at its end; it is assumed to be small. The velocities of these vectors are correspondingly written as

$$\dot{\mathbf{r}}_1 = \dot{v}_1\, \mathbf{a}_2 \tag{5}$$

and

$$\dot{\mathbf{r}}_2 = -(x_2\, \dot{\alpha} \sin(\theta) + \dot{v}_2 \sin(\theta))\mathbf{a}_1 + (\dot{v}_1(L_1, t) + x_2\, \dot{\alpha} \cos(\theta) + \dot{v}_2 \cos(\theta))\mathbf{a}_2. \tag{6}$$

Note that non-linear or second order terms (i.e., $\alpha\dot{\alpha}$ and $v_2\, \dot{\alpha}$) have been ignored in writing equation (6).

The system kinetic energy T is composed of three components, the contributions from the beams and the contribution of the tip mass, so that

$$T = T_1 + T_2 + T_t, \tag{7}$$

where

$$T_k = \tfrac{1}{2} \int_0^{L_k} \rho_k\, A_k\, \dot{\mathbf{r}}_k \cdot \dot{\mathbf{r}}_k\, \mathrm{d}x_k \qquad \text{for } k = 1, 2 \tag{8}$$

and

$$T_t = \tfrac{1}{2}\, m_t\, \dot{\mathbf{r}}_2(L_2, t) \cdot \dot{\mathbf{r}}_2(L_2, t). \tag{9}$$

The system potential energy U is composed of a contribution from each beam segment and is given by

$$U = \tfrac{1}{2} \int_0^{L_1} E_1\, I_1\, (\partial^2 v_1 / \partial x_1^2)^2\, \mathrm{d}x_1 + \tfrac{1}{2} \int_0^{L_2} E_2\, I_2\, (\partial^2 v_2 / \partial x_2^2)^2\, \mathrm{d}x_2. \tag{10}$$

TABLE 1

Material properties and non-dimensional parameters

Parameter	Value
L_1	4·249 m
L_2	2·215 m
L	0·5213
$\rho_1 A_1$	$4{\cdot}5 \times 10^{-3}$ kg m^{-1}
$\rho_2 A_2$	$6{\cdot}0 \times 10^{-3}$ kg m^{-1}
ρ	1·333
$E_1 I_1$	$2{\cdot}67 \times 10^{-2}$ N m^2
$E_2 I_2$	$1{\cdot}47 \times 10^{-2}$ N m^2
λ_1	$54{\cdot}93\omega^2$
λ_2	$9{\cdot}825\omega^2$

Using T and U in Hamilton's principle and taking variations over the displacements v_1 and v_2, the following equations of motion are obtained:

$$\rho_1 A_1 \ddot{v}_1 + E_1 I_1 (\partial^4 v_1 / \partial x_1^4) = 0 \tag{11}$$

and

$$\rho_2 A_2 (\ddot{v}_2 + x_2 \ddot{\alpha} + \ddot{v}_1 (L_1, t) \cos(\theta)) + E_2 I_2 (\partial^4 v_2 / \partial x_2^4) = 0. \tag{12}$$

The corresponding boundary conditions are

$$v_1 (x_1, t)|_{x_1 = 0} = 0, \qquad v_1' (x_1, t)|_{x_1 = 0} = 0, \qquad v_2 (x_2, t)|_{x_2 = 0} = 0, \tag{13–15}$$

$$v_2' (x_2, t)|_{x_2 = 0} = 0, \qquad v_2'' (x_2, t)|_{x_2 = L_2} = 0, \tag{16, 17}$$

$$m_t (\ddot{v}_2 (L_2, t) + L_2 \ddot{\alpha} + \ddot{v}_1 (L_1, t) \cos(\theta)) = E_2 I_2 v_2''' (L_2, t), \tag{18}$$

TABLE 2

Analytical natural frequencies, $\omega_i (s^{-1})$

M_t	Mode	$\theta = 0$	$\theta = \pi/6$	$\theta = \pi/3$	$\theta = \pi/2$ (present)	$\theta = \pi/2$ (Bang [13])	$\theta = 2\pi/3$	$\theta = 5\pi/6$	$\theta = \pi$
0·0	ω_1	0·1807	0·1852	0·1994	0·2247	2·2419	0·2608	0·2968	0·3117
	ω_2	1·1489	1·0639	0·9068	0·7940	14·3003	0·7636	0·8370	0·9248
	ω_3	2·9705	2·8758	2·7442	2·6814	19·7509	2·6847	2·7655	2·8582
	ω_4	6·0755	5·9631	5·8052	5·7715	24·3269	5·9304	6·5497	7·4101
	ω_5	9·8732	9·1043	8·3684	8·0768	37·0270	7·9638	7·9427	8·0954
0·1	ω_1	0·1642	0·1686	0·1827	0·2088		0·2484	0·2903	0·3076
	ω_2	1·0442	0·9504	0·7863	0·6701		0·6265	0·6718	0·7412
	ω_3	2·7557	2·6964	2·6182	2·5905		2·6199	2·7345	2·8568
	ω_4	5·7112	5·4868	5·1936	5·0852		5·1643	5·6129	6·3125
	ω_5	9·2382	8·5727	8·0184	7·8243		7·7688	7·8320	8·0936
0·2	ω_1	0·1514	0·1557	0·1695	0·1957		0·2374	0·2841	0·3031
	ω_2	0·9839	0·8814	0·7114	0·5943		0·5447	0·5770	0·6411
	ω_3	2·6600	2·6115	2·5522	2·5379		2·5777	2·7103	2·8561
	ω_4	5·5701	5·2877	4·9497	4·8241		4·8751	5·2597	5·9394
	ω_5	9·0424	8·3911	7·9029	7·7444		7·7077	7·7928	8·0934
0·3	ω_1	0·1412	0·1453	0·1587	0·1847		0·2277	0·2783	0·2982
	ω_2	0·9449	0·8339	0·6587	0·5415		0·4891	0·5138	0·5774
	ω_3	2·6069	2·5620	2·5111	2·5030		2·5468	2·6896	2·8557
	ω_4	5·4972	5·1746	4·8184	4·6896		4·7265	5·0718	5·7529
	ω_5	8·9501	8·2896	7·8384	7·7002		7·6728	7·7657	8·0934
0·4	ω_1	0·1327	0·1367	0·1497	0·1753		0·2190	0·2727	0·2929
	ω_2	0·9178	0·7985	0·6187	0·5022		0·4481	0·4680	0·5333
	ω_3	2·5732	2·5293	2·4827	2·4777		2·5227	2·6714	2·8554
	ω_4	5·4529	5·0985	4·7348	4·6078		4·6362	4·9528	5·6412
	ω_5	8·8967	8·2195	7·7944	7·6703		7·6485	7·7439	8·0933
0·5	ω_1	0·1256	0·1295	0·1421	0·1671		0·2112	0·2674	0·2872
	ω_2	0·8979	0·7704	0·5866	0·4712		0·4164	0·4328	0·5012
	ω_3	2·5501	2·5059	2·4617	2·4583		2·5033	2·6550	2·8552
	ω_4	5·4232	5·0417	4·6761	4·5528		4·5756	4·8693	5·5668
	ω_5	8·8620	8·1657	7·7614	7·6480		7·6299	7·7255	8·0933

$$\int_0^{L_2} \rho_2 A_2 x_2 (\ddot{v}_2 + x_2 \ddot{\alpha} + \ddot{v}_1 (L_1, t) \cos(\theta)) \, dx_2 + m_t L_2 (L_2 \ddot{\alpha} + \ddot{v}_2 (L_2, t) + \ddot{v}_1 (L_1, t) \cos(\theta)) = -E_1 I_1 v_1'' (L_1, t), \quad (19)$$

$$\int_0^{L_2} \rho_2 A_2 (\ddot{v}_1 (L_1, t) + (\ddot{v}_2 + x_2 \ddot{\alpha}) \cos(\theta)) \, dx_2 + m_t (\ddot{v}_1 (L_1, t) + (\ddot{v}_2 (L_2, t) + L_2 \ddot{\alpha}) \cos(\theta)) = E_1 I_1 v_1''' (L_1, t). \quad (20)$$

4. FREQUENCY EQUATION

To reduce the number of defining parameters we introduce the non-dimensional variables:

$$\xi_i = x_i / L_i, \qquad \rho = \rho_2 A_2 / \rho_1 A_1, \qquad \lambda_i^4 = \rho_i A_i L_i^4 \omega^2 / E_i I_i,$$
$$M_t = m_t / \rho_1 A_1 L_1, \qquad L = L_2 / L_1. \quad (21)$$

TABLE 3

Finite element analysis natural frequencies, $\omega_i (s^{-1})$

M_t	Mode	$\theta = 0$	$\theta = \pi/6$	$\theta = \pi/3$	$\theta = \pi/2$	$\theta = 2\pi/3$	$\theta = 5\pi/6$	$\theta = \pi$
0·0	ω_1	0·1807	0·1852	0·1994	0·2247	0·2608	0·2968	0·3117
	ω_2	1·1489	1·0639	0·9068	0·7940	0·7636	0·8370	0·9248
	ω_3	2·9705	2·8758	2·7442	2·6814	2·6847	2·7655	2·8582
	ω_4	6·0756	5·9632	5·8053	5·7716	5·9305	6·5498	7·4104
	ω_5	9·8736	9·1045	8·3685	8·0770	7·9638	7·9428	8·0855
0·1	ω_1	0·1642	0·1686	0·1827	0·2088	0·2484	0·2903	0·3076
	ω_2	1·0442	0·9504	0·7863	0·6701	0·6265	0·6718	0·7412
	ω_3	2·7557	2·6964	2·6182	2·5905	2·6199	2·7345	2·8568
	ω_4	5·7112	5·4869	5·1936	5·0852	5·1643	5·6130	6·3126
	ω_5	9·2385	8·5728	8·0185	7·8244	7·7690	7·8321	8·0938
0·2	ω_1	0·1514	0·1557	0·1695	0·1957	0·2374	0·2841	0·3031
	ω_2	0·9839	0·8814	0·7114	0·5943	0·5447	0·5770	0·6411
	ω_3	2·6600	2·6115	2·5522	2·5379	2·5777	2·7103	2·8561
	ω_4	5·5702	5·2877	4·9498	4·8241	4·8752	5·2597	5·9395
	ω_5	9·0427	8·3912	7·9030	7·7445	7·7079	7·7929	8·0936
0·3	ω_1	0·1412	0·1453	0·1587	0·1847	0·2277	0·2783	0·2982
	ω_2	0·9449	0·8339	0·6587	0·5416	0·4891	0·5138	0·5774
	ω_3	2·6069	2·5620	2·5111	2·5030	2·5468	2·6896	2·8557
	ω_4	5·4972	5·1747	4·8184	4·6896	4·7265	5·0718	5·7530
	ω_5	8·9504	8·2897	7·8385	7·7003	7·6729	7·7658	8·0935
0·4	ω_1	0·1327	0·1367	0·1497	0·1753	0·2190	0·2727	0·2929
	ω_2	0·9178	0·7985	0·6186	0·5022	0·4481	0·4680	0·5333
	ω_3	2·5732	2·5293	2·4827	2·4777	2·5227	2·6714	2·8554
	ω_4	5·4529	5·0985	4·7348	4·6079	4·6362	4·9528	5·6413
	ω_5	8·8970	8·2197	7·7945	7·6704	7·6486	7·7440	8·0935
0·5	ω_1	0·1256	0·1295	0·1421	0·1671	0·2112	0·2674	0·2872
	ω_2	0·8979	0·7703	0·5866	0·4711	0·4163	0·4328	0·5012
	ω_3	2·5501	2·5058	2·4616	2·4583	2·5033	2·6550	2·8552
	ω_4	5·4232	5·0416	4·6761	4·5528	4·5756	4·8693	5·5668
	ω_5	8·8623	8·1658	7·7614	7·6481	7·6300	7·7256	8·0935

By assuming a separable solution in the form

$$v_i(x_i, t) = L_i V_i(\xi_i) e^{i\omega t} \qquad \text{for } i = 1, 2, \tag{22}$$

the equations of motion can be written as

$$V_1'''' - \lambda_1^4 V_1 = 0 \tag{23}$$

and

$$V_2'''' - \lambda_2^4 \left(V_2 - \xi_2 V_1'(1) + \frac{1}{L} V_1(1) \cos(\theta) \right) = 0. \tag{24}$$

With non-dimensionalization and separation of variables, the boundary conditions can be expressed as

$$V_1(0) = 0, \qquad V_1'(0) = 0, \qquad V_2(0) = 0, \qquad V_2'(0) = 0, \qquad V_2''(1) = 0, \tag{25–29}$$

$$\lambda_2^4 M_t \left(V_2(1) + V_1'(1) + \frac{1}{L} V_1(1) \cos(\theta) \right) = -\rho L V_2'''(1), \tag{30}$$

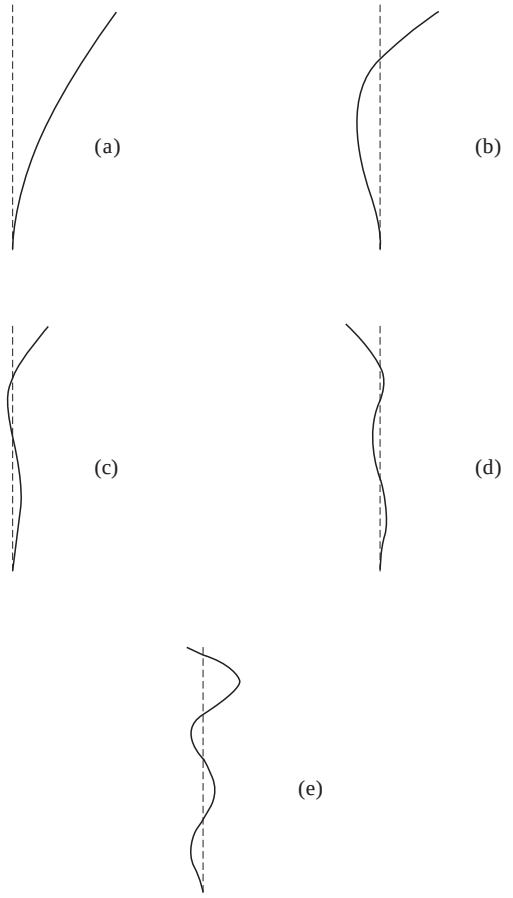

Figure 2. Mode shapes of the structure for $\theta = 0$. ---, Undeformed; —, deformed. (a) first mode; (b) second mode; (c) third mode; (d) fourth mode; (e) fifth mode.

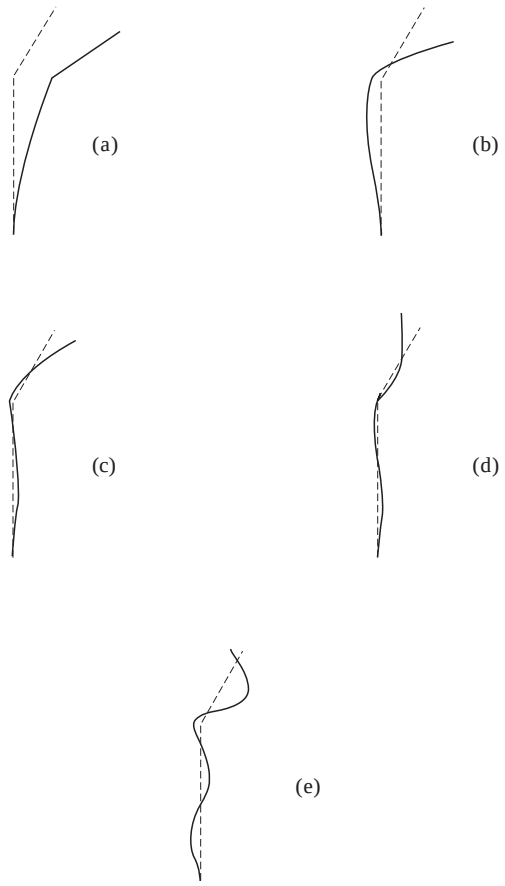

Figure 3. Mode shapes of the structure for $\theta = \pi/6$. ---, Undeformed; —, deformed. (a) first mode; (b) second mode; (c) third mode; (d) fourth mode; (e) fifth mode.

$$\lambda_1^4 \rho L^3 \int_0^1 \xi_2 \left(V_2 + \xi_2 V_1'(1) + \frac{1}{L} V_1(1) \cos(\theta) \right) \mathrm{d}\xi_2 + \lambda_1^4 M_t L^2 \left(V_1'(1) + V_2(1) + \frac{1}{L} V_1(1) \cos(\theta) \right) = V_1''(1), \tag{31}$$

$$\lambda_1^4 \rho L^2 \int_0^1 \left(\frac{1}{L} V_1(1) + (V_2 + \xi_2 V_1'(1)) \cos(\theta) \right) \mathrm{d}\xi_2 + \lambda_1^4 M_t L \left(\frac{1}{L} V_1(1) + (V_2(1) + V_1'(1)) \cos(\theta) \right) = -V_1'''(1). \tag{32}$$

The general solution to the equation of motion (23) is

$$V_1(\xi_1) = B_1 \sin(\lambda_1 \xi_1) + B_2 \cos(\lambda_1 \xi_1) + B_3 \sinh(\lambda_1 \xi_1) + B_4 \cosh(\lambda_1 \xi_1) \tag{33}$$

and the general solution to equation (24) is

$$V_2(\xi_2) = C_1 \sin(\lambda_2 \xi_2) + C_2 \cos(\lambda_2 \xi_2) + C_3 \sinh(\lambda_2 \xi_2) + C_4 \cosh(\lambda_2 \xi_2)$$

$$-\left(\xi_2 V_1'(1) + \frac{1}{L} V_1(1) \cos(\theta)\right). \tag{34}$$

From equations (25) and (26) we have that

$$B_2 = -B_4 \qquad \text{and} \qquad B_1 = -B_3, \tag{35}$$

respectively, and hence equation (33) can be rewritten as

$$V_1(\xi_1) = B_1(\sin(\lambda_1 \xi_1) - \sinh(\lambda_1 \xi_1)) + B_2(\cos(\lambda_1 \xi_1) - \cosh(\lambda_1 \xi_1)). \tag{36}$$

We now substitute equations (34) and (36) into the remaining boundary conditions (i.e., equations (27)–(32)) and after some algebra obtain six homogeneous equations which are linear in the unknown coefficients of integration. These equations can be expressed in matrix format as

$$[A]_{6\times 6}\{q\}_{6\times 1} = \{0\}_{6\times 1}, \tag{37}$$

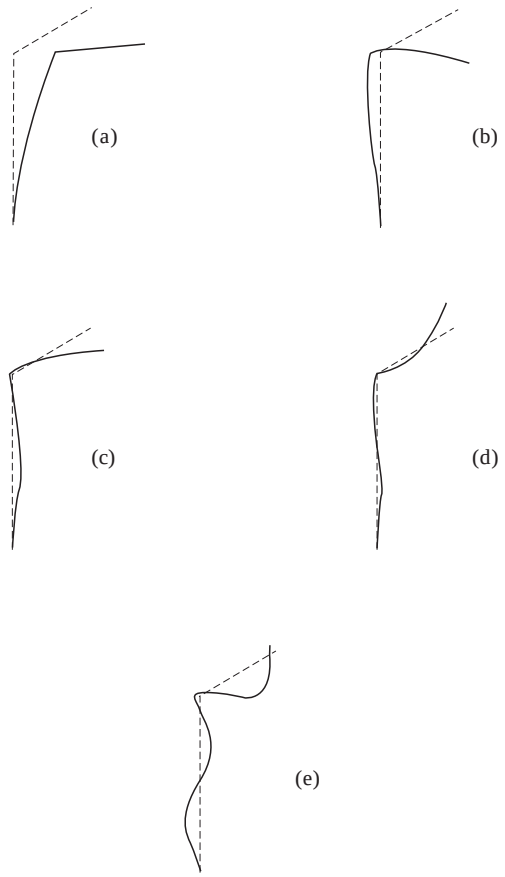

Figure 4. Mode shapes of the structure for $\theta = \pi/3$. ---, Undeformed; —, deformed. (a) first mode; (b) second mode; (c) third mode; (d) fourth mode; (e) fifth mode.

where the elements of the matrix A are listed in Appendix B, and $\{q\} = [B_1, B_2, C_1, C_2, C_3, C_4]^{\mathrm{T}}$.

A non-trivial solution is found by setting the determinant of the matrix to zero, to yield the frequency equation:

$$\begin{aligned}
&\rho L\lambda_2\,(\lambda_2^3\mathbf{F}_{cf1}\,\mathbf{F}_{cf2} - \rho L^3\lambda_1^3\mathbf{F}_{cr1}\,\mathbf{F}_{cs2})\\
&\quad - \rho^2L^2\lambda_1\,\lambda_2\,(\lambda_2^3\mathbf{F}_{cs1}\,\mathbf{F}_{cf2} - \rho L^3\lambda_1^3\mathbf{F}_{cc1}\,\mathbf{F}_{cs2})\sin^2(\theta)\\
&\quad - \rho^2L^2\lambda_1\,(\lambda_2^3\mathbf{F}_{cs1}\,\mathbf{F}_{cr2} - \rho L^3\lambda_1^3\mathbf{F}_{cc1}\,\mathbf{F}_{cc2})\cos^2(\theta)\\
&\quad - 2\rho^2L^3\lambda_1^2\lambda_2^2\mathbf{F}_{ss1}\,\mathbf{F}_{ss2}\cos(\theta)\\
&\quad + \lambda_1\,\lambda_2^2(\lambda_2^3\mathbf{F}_{cs1}\,\mathbf{F}_{cs2} + 2\rho L^3\lambda_1^3\mathbf{F}_{cc1}\,\mathbf{F}_{ss2})M_t^2\sin^2(\theta)\\
&\quad - 2\rho L^2\lambda_1^2\lambda_2^3\mathbf{F}_{ss1}\,\mathbf{F}_{cr2}\,M_t\cos(\theta)\\
&\quad + \rho L\lambda_1\,\lambda_2^2(\lambda_2^3\mathbf{F}_{cs1}\,\mathbf{F}_{cs2} + 2\rho L^3\lambda_1^3\mathbf{F}_{cc1}\,\mathbf{F}_{ss2})M_t\sin^2(\theta)\\
&\quad + \rho L\lambda_1\,\lambda_2^4\mathbf{F}_{cs1}\,\mathbf{F}_{cc2}\,M_t\cos^2(\theta)\\
&\quad - \lambda_2\,(\lambda_2^4\mathbf{F}_{cf1}\,\mathbf{F}_{cs2} + \rho L\lambda_1\,(\lambda_2^3\mathbf{F}_{cs1}\,\mathbf{F}_{cf2}\\
&\quad - L^2\lambda_1^2(\rho L\lambda_1\,\mathbf{F}_{cc1}\,\mathbf{F}_{cs2} - 2\lambda_2\,\mathbf{F}_{cr1}\,\mathbf{F}_{ss2})))M_t = 0,
\end{aligned} \tag{38}$$

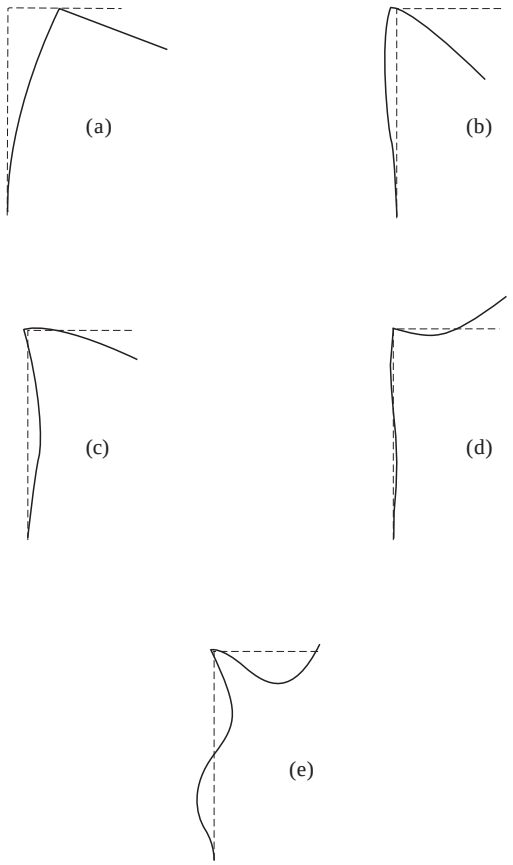

Figure 5. Mode shapes of the structure for $\theta = \pi/2$. ---, Undeformed; —, deformed. (a) first mode; (b) second mode; (c) third mode; (d) fourth mode; (e) fifth mode.

where

$$\mathbf{F}_{cci} = 1 - \cos(\lambda_i)\cosh(\lambda_i), \qquad \mathbf{F}_{csi} = \sin(\lambda_i)\cosh(\lambda_i) - \cos(\lambda_i)\sinh(\lambda_i),$$
$$\mathbf{F}_{ssi} = \sin(\lambda_i)\sinh(\lambda_i), \qquad \mathbf{F}_{cri} = \sin(\lambda_i)\cosh(\lambda_i) + \cos(\lambda_i)\sinh(\lambda_i),$$
$$\mathbf{F}_{sri} = \cos(\lambda_i)\cosh(\lambda_i), \qquad \mathbf{F}_{cfi} = 1 + \cos(\lambda_i)\cosh(\lambda_i). \tag{39}$$

In the last six relations, a subscript c denotes a clamped end, an f represents a free end, a r represents a roller end, and an s donates a supported end. The subscripts 1 and 2 indicate whether the reference is to the first or the second beam. Each $\mathbf{F}\ldots$ corresponds to the frequency equation for a single beam with the boundary conditions indicated by the subscripts. (i.e., $\mathbf{F}_{cf1} = 0$ is the frequency equation for a clamped–free (cantilever) beam with properties of the first beam). It may be observed that equation (38) is symmetric about $\theta = 0$, (i.e., it will be the same for both positive and negative values of θ).

For an L-shaped arrangement with no tip mass (i.e., $M_t = 0$ and $\theta = \pi/2$), the frequency equation (38) becomes

$$\lambda_2^3 \mathbf{F}_{cf2}(\mathbf{F}_{cf1} - \rho L\lambda_1 \mathbf{F}_{cs1}) - \rho L^3 \lambda_1^3 \mathbf{F}_{cs2}(\mathbf{F}_{cr1} - \rho L\lambda_1 \mathbf{F}_{cc1}) = 0. \tag{40}$$

This equation is different from equation (14) in Bang [13], presumably because of possible errors in that work. These are detailed in section 7.

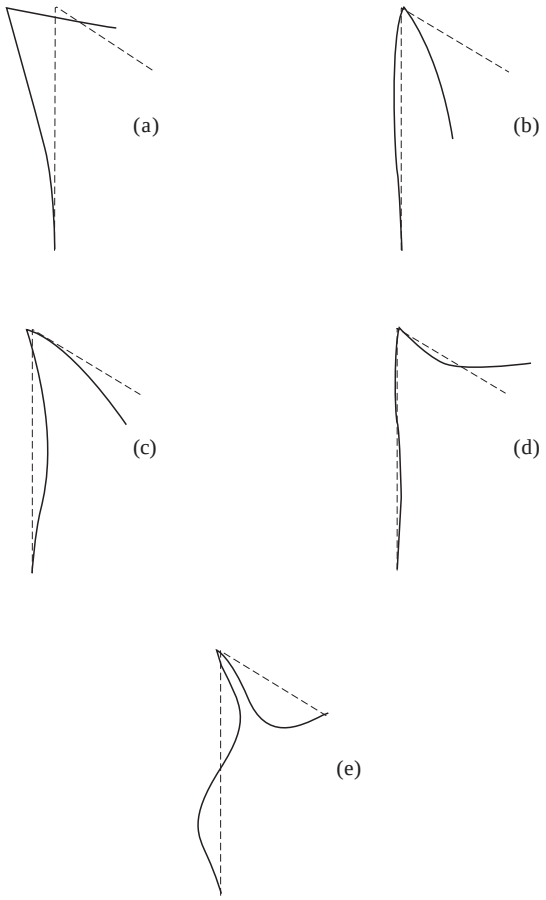

Figure 6. Mode shapes of the structure for $\theta = 2\pi/3$. ---, Undeformed; —, deformed. (a) first mode; (b) second mode; (c) third mode; (d) fourth mode; (e) fifth mode.

5. MODE SHAPES

The mode shapes are derived by using the shear and moment conditions at the end of the second beam, equations (29) and (30), the slope and displacement conditions at the base of the second beam, equations (27) and (28), and the moment condition of the end of the first beam, equation (31). With reference to equations (33)–(35) the coefficients of the mode shapes are

$$B_1 = C_4 [2L\lambda_2^3(\cos(\lambda_1) + \cosh(\lambda_1))(\rho L\mathbf{F}_{cf2} - \lambda_2 M_t \mathbf{F}_{cs2}) - 2\rho L^4\lambda_1^3(\sin(\lambda_1) + \sinh(\lambda_1))(\rho L\mathbf{F}_{cs2} + 2\lambda_2 M_t \mathbf{F}_{ss2}) + 2\rho L^3\lambda_1^2\lambda_2(\cos(\lambda_1) - \cosh(\lambda_1))(\rho L\mathbf{F}_{ss2} + \lambda_2 M_t \mathbf{F}_{cr2})\cos(\theta)]/\Delta, \quad (41)$$

$$B_2 = C_4 [-2L\lambda_2^3(\sin(\lambda_1) + \sinh(\lambda_1))(\rho L\mathbf{F}_{cf2} - \lambda_2 M_t \mathbf{F}_{cs2}) - 2\rho L^4\lambda_1^3(\cos(\lambda_1) - \cosh(\lambda_1))(\rho L\mathbf{F}_{cs2} + 2\lambda_2 M_t \mathbf{F}_{ss2}) - 2\rho L^3\lambda_1^2\lambda_2(\sin(\lambda_1) - \sinh(\lambda_1))(\rho L\mathbf{F}_{ss2} + \lambda_2 M_t \mathbf{F}_{cr2})\cos(\theta)]/\Delta, \quad (42)$$

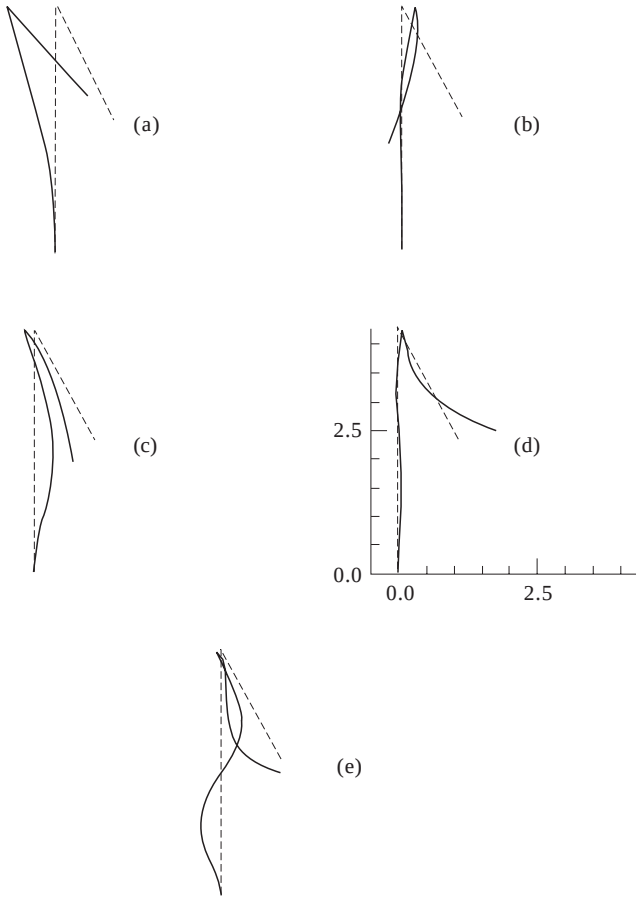

Figure 7. Mode shapes of the structure for $\theta = 5\pi/6$. ---, Undeformed; —, deformed. (a) first mode; (b) second mode; (c) third mode; (d) fourth mode; (e) fifth mode.

$$C_1 = C_4\,[2\rho L^2\lambda_1\,\lambda_2^2\mathbf{F}_{ss1}\,(\mathbf{F}_{cf2} + \mathbf{F}_{ss2}) + 4L\lambda_1\,\lambda_2^3\cos(\lambda_2)\sinh(\lambda_2)\mathbf{F}_{ss1}\,M_t$$
$$+ 2\rho L(\lambda_2^3\mathbf{F}_{cs1}\,\mathbf{F}_{cr2} + \rho L^3\lambda_1^3\mathbf{F}_{cc1}\,(\mathbf{F}_{ss2} - \mathbf{F}_{cc2}))\cos(\theta)$$
$$+ 4\lambda_2\,(\lambda_2^3\mathbf{F}_{cs1}\,\mathbf{F}_{sr2} + \rho L^3\lambda_1^3\cos(\lambda_2)\sinh(\lambda_2)\mathbf{F}_{cc1})M_t\cos(\theta)]/\Delta, \tag{43}$$

$$C_2 = C_4\,[-2\rho L^2\lambda_1\,\lambda_2^2\mathbf{F}_{ss1}\,\mathbf{F}_{cs2} - 4L\lambda_1\,\lambda_2^3\mathbf{F}_{ss1}\,\mathbf{F}_{ss2}\,M_t$$
$$+ 2\rho L(\lambda_2^3\mathbf{F}_{cs1}\,(\mathbf{F}_{cf2} - \mathbf{F}_{ss2}) - \rho L^3\lambda_1^3\mathbf{F}_{cc1}\,\mathbf{F}_{cs2})\cos(\theta)$$
$$- 4\lambda_2\,(\lambda_2^3\sin(\lambda_2)\cosh(\lambda_2)\mathbf{F}_{cs1} + \rho L^3\lambda_1^3\mathbf{F}_{cc1}\,\mathbf{F}_{ss2})M_t\cos(\theta)/\Delta, \tag{44}$$

$$C_3 = C_4\,[2\rho L^2\lambda_1\,\lambda_2^2\mathbf{F}_{ss1}\,(\mathbf{F}_{cf2} - \mathbf{F}_{ss2}) - 4L\lambda_2^4\mathbf{F}_{cs1}\,\mathbf{F}_{sr2}\,M_t$$
$$- 2\rho L(\lambda_2^3\mathbf{F}_{cs1}\,\mathbf{F}_{cr2} - \rho L^3\lambda_1^3\mathbf{F}_{cc1}\,(\mathbf{F}_{cc2} + \mathbf{F}_{ss2}))\cos(\theta)$$
$$- 4\lambda_2\,(\lambda_2^3\mathbf{F}_{cs1}\,\mathbf{F}_{sr2} - \rho L^3\lambda_1^3\sin(\lambda_2)\cosh(\lambda_2)\mathbf{F}_{cc1})M_t\cos(\theta)]/\Delta, \tag{45}$$

where

$$\Delta = 2\rho L^2\lambda_1\,\lambda_2^2\mathbf{F}_{ss1}\,\mathbf{F}_{cs2} + 4L\lambda_1\,\lambda_2^3\mathbf{F}_{ss1}\,\mathbf{F}_{ss2}\,M_t$$
$$+ 2\rho L(\lambda_2^3\mathbf{F}_{cs1}\,(\mathbf{F}_{ss2} + \mathbf{F}_{cf2}) - \rho L^3\lambda_1^3\mathbf{F}_{cc1}\,\mathbf{F}_{cs2})\cos(\theta)$$
$$+ 4\lambda_2\,(\lambda_2^3\cos(\lambda_2)\sinh(\lambda_2)\mathbf{F}_{cs1} - \rho L^3\lambda_1^3\mathbf{F}_{cc1}\,\mathbf{F}_{ss2})M_t\cos(\theta). \tag{46}$$

Examples of the first five mode shapes are presented in section 7.

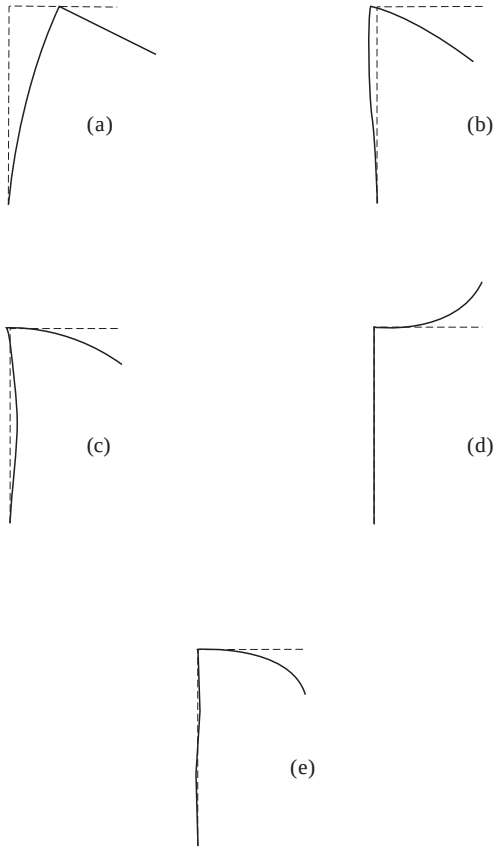

Figure 8. Mode shapes of the structure for $\theta = \pi/2$ and $M_t = 0{\cdot}2$. ---, Undeformed; —, deformed. (a) first mode; (b) second mode; (c) third mode; (d) fourth mode; (e) fifth mode.

6. ORTHOGONALITY CONDITION

The orthogonality condition is derived using the non-dimensional equations of motion, equations (23) and (24), and the corresponding non-dimensional boundary conditions, equations (25)–(32). The resulting orthogonality condition may be expressed as

$$\int_0^1 V_{1i}\,V_{1j}\,\mathrm{d}\xi_1 + \rho L V_{1i}(1)V_{1j}(1) + \frac{\rho L^3}{3}\,V'_{1i}(1)V'_{1j} \tag{1}$$

$$+\,\rho L^3 \int_0^1 (V_{2i}\,V_{2j} + \xi_2\,(V_{2i}\,V'_{1j}(1) + V_{2j}\,V'_{1i}(1)))\,\mathrm{d}\xi_2$$

$$+\,\rho L^2\left(\tfrac{1}{2}\,(V_{1i}(1)V'_{1j}(1) + V_{1j}(1)V'_{1i}(1)) + \int_0^1 (V_{1j}(1)V_{2i} + V_{1i}(1)V_{2j})\,\mathrm{d}\xi_2\right)\cos(\theta)$$

$$+\,(V_{1i}(1)V_{1j}(1) + L^2(V'_{1j}(1)V'_{1i}(1) + V_{2i}(1)V_{2j}(1) + V_{2i}(1)V'_{1j} + V_{2j}(1)V'_{1i}))M_t$$

$$+\,L(V_{1i}(1)V'_{1j}(1) + V_{1j}(1)V'_{1i} + V_{1i}(1)V_{2j}(1) + V_{1j}(1)V_{2i}(1))M_t\cos(\theta) = 0, \qquad i \neq j. \tag{47}$$

This equation has been written so that the contributions of the tip mass and the effect of the angle of displacement from the vertical are readily observed.

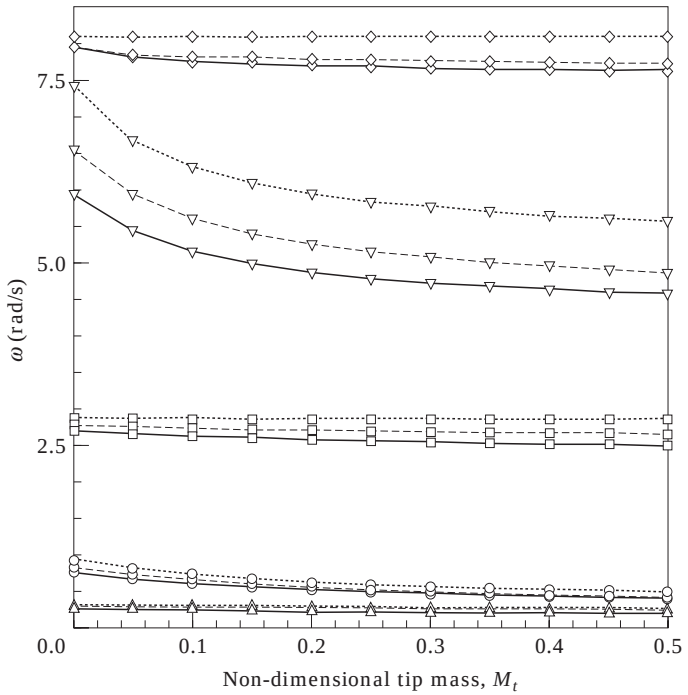

Figure 9. The fifth effect of the tip mass on the natural frequencies for $\theta = \pi/6$ —, $\pi/3$ --- and $\pi/2$ . . . . △, first mode; ○, second mode; □, third mode; ▽, fourth mode; ◇ fifth mode.

7. NUMERICAL EXAMPLES

The material properties tabulated in Table 1 have been taken from Bang [13] in order to permit comparison of results. The system is simulated with and without a payload, and the displacement of the second beam from the vertical is varied from 0 to 180°. The natural frequencies, as determined by numerically solving for the roots of the frequency equation (38) are displayed in Table 2 and a corresponding set of natural frequencies as obtained from a 20-element (ten elements in each beam) finite element model are given in Table 3. Comparison of the data in these two tables shows that the natural frequency values are identical to within five significant digits for the first four natural frequencies and to within four significant digits for the fifth natural frequency; an agreement that gives confidence in the results. We did not experience any numerical difficulties in obtaining the roots of the frequency equation in spite of its complexity and the presence of hyperbolic functions. Accurately finding a large number of frequencies can be done with greater computational economy by solving equation (38) than by solving the necessarily large eigenvalue problem associated with a finite element model. Indeed, one of the attributes of equation (38) is that it can be used to help verify the finite element code and model.

Using the material properties given in Table 1, the first five modes of the structure with no payload at the tip of the beam and the orientation angle $\theta = 0°$, 30°, 60°, 90°, 120° and 150° are depicted in Figures 2–7, respectively. The mode shapes for a 90° configuration with a tip mass ($M_t = 0{\cdot}2$) are presented in Figure 8. We cannot make any general conclusions on the basis of these figures, as the mode shapes will vary according to the relative length L, relative linear mass density ρ and relative λ_i values for the structure. However, there are some features in these figures which are of note. The most striking feature is the very small participation of the second beam in the first mode, regardless of

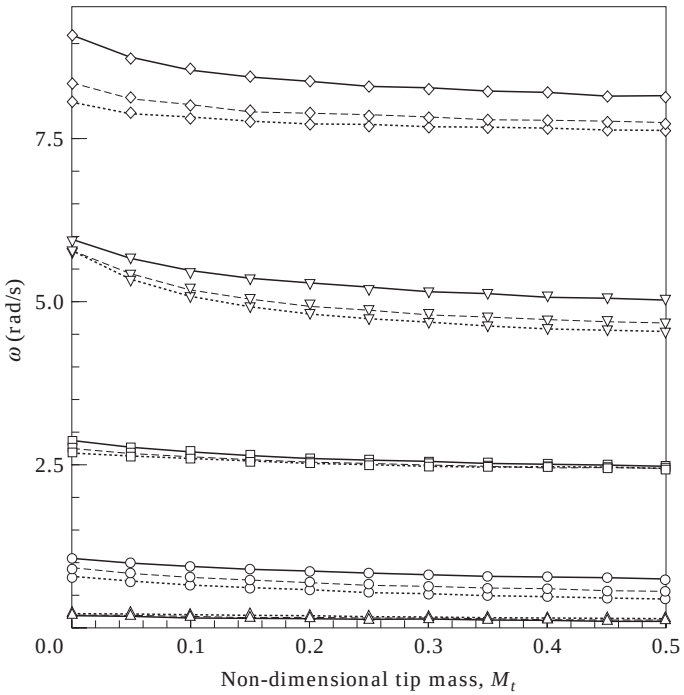

Figure 10. The effect of the tip mass on the natural frequencies for $\theta = 2\pi/3$ —, $5\pi/6$ --- and π . . . . . △, first mode; ○, second mode; □, third mode; ▽, fourth mode; ◇ fifth mode.

the value of θ. For this set of materials and geometry parameters, the first mode is dominated by a simple cantilever mode in the first beam.

A comparison of the mode shapes presented in Figures 5 and 8 gives some indication of the effect that the presence of a tip mass can have. The first three mode shapes are not markedly different between the two cases, but the fourth and fifth mode shapes are quite different. For the case investigated here, the presence of the tip mass has resulted in the first beam having a diminished contribution in the fourth and fifth modes, which are now dominated by the second beam.

For a given angle of inclination, each of the first five modes displays declining frequency values with increasing tip mass, as may be observed in Table 2 and Figures 9 and 10. This is an intuitively appealing result that parallels the well known results for straight uniform beams with tip masses [14].

Another perspective on the results presented in Figures 9 and 10 is available in Figure 11, which shows the effect of the angle of inclination on the natural frequencies (with and without a tip mass).

For any fixed tip mass value, the first natural frequency (see Table 2 and Figure 11) rises from its value at $\theta = 0$ to a larger value at $\theta = \pi$. We can see in Figures 2–8 that the distal (second) beam does not participate in the first mode and, consequently, we might reasonably expect to see the frequency behave as a single cantilever beam with a constant stiffness (EI) but with a monotonically declining (with θ) system inertia. This would result in the behavior exhibited by $\omega_1(\theta)$. In contrast, the higher modal frequencies display a concave upward behavior as θ is varied from $\theta = \pi/6$ to $\theta = \pi$ for a constant value of the tip mass (see Figure 11). The minimum value in each row of Table 2 is underlined, and we can see in that data that the location of the minimum for the second mode is in the vicinity of $\theta = 2\pi/3$. For the third and fourth modes the minimum frequency occurs in the vicinity of $\theta = \pi/2$, while the minimum frequency for the fifth mode is, like the second mode, near $\theta = 2\pi/3$ for larger values of the tip mass but is near $\theta = 5\pi/6$ for the case in which there is no tip mass. It is evident from Figures 2–8 that the distal beam does have a significant contribution to the higher mode shapes, and an explanation based on intuitive

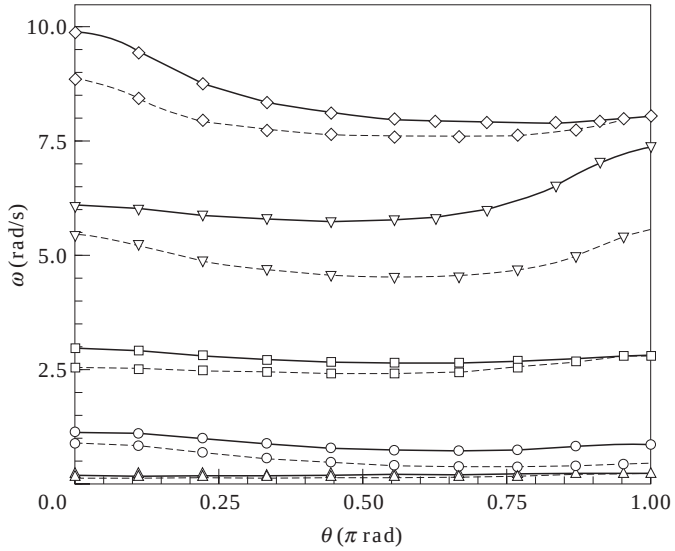

Fig. 11. The effect of inclination on the natural frequencies. —— $M_t = 0$; – – –, $M_t = 0.5$. △, first mode; ○, second mode; □, third mode; ▽, fourth mode; ◇, fifth mode.

arguments about the stiffness and inertia is not going to provide a satisfactory explanation of this behavior.

Finally, we would like to explain the wide discrepancies between our results and those reported by Bang [13] for the L-shaped arrangement. As stated in an earlier section, the differences are probably attributable to possible errors in the elements of the matrix which are coefficients of the unknown variables. In particular, the matrix entries A_{53}, A_{54} and A_{55} should be, in our opinion,

$$A_{53} = \{\}\rho_2\,\omega^2[(1/\gamma_2^2)\sin\gamma_2\,l_2 - (l_2/\gamma_2)\cos\gamma_2\,l_2],$$

$$A_{54} = \{\}\rho_2\,\omega^2[(1/\gamma_2^2)\cos\gamma_2\,l_2 + (l_2/\gamma_2)\sin\gamma_2\,l_2\,(-2/\gamma_2^2) - (l_2/\gamma_2)\sinh\gamma_2\,l_2 + (1/\gamma_2^2)\cosh\gamma_2\,l_2]$$

and

$$A_{55} = \{\}\rho_2\,\omega^2[(l_2/\gamma_2)\cosh\gamma_2\,l_2 - (1/\gamma_2^2)\sinh\gamma_2\,l_2],$$

respectively. The $-2/\gamma_2^2$ term is missing in reference [13] and $\{\}$ contained minus signs.

8. SUMMARY

Hamilton's principle has been used to obtain the equations of motion of a generalized two-beam open frame structure. The generalization was achieved through the attachment of a payload at the tip of one flexible beam, and the arbitrary planar orientation of the distal beam relative to the base beam. The reported frequency equation, mode shapes and orthogonal condition are indicative of the coupling and complexity that is inherent in the system. The mode shapes corresponding to the lowest natural frequency have very little participation from the distal beam and the first mode is dominated by the cantilever like motion of the base beam.

The numerical examples indicate that the dependence of the frequencies on the angle of inclination is much more complicated than their dependence on the value of the tip mass.

REFERENCES

1. N. F. Rieger and H. McCallion 1965 *International Journal of Mechanical Science* **7**, 253–261. The natural frequencies of portal frames—I.
2. N. F. Rieger and H. McCallion 1965 *International Journal of Mechanical Science* **7**, 263–276. The natural frequencies of portal frames—II.
3. C. P. Filipich, B. H. Valerga de Greco and P. A. A. Laura 1987 *Journal of Sound and Vibration* **117**, 198–201. A note on the analysis of symmetric mode of vibrations of portal frames.
4. P. A. A. Laura and B. H. Valerga de Greco 1987 *Journal of Sound and Vibration* **117**, 447–458. In-plane vibrations of frames carrying concentrated masses.
5. C. P. Filipich and P. A. A. Laura 1987 *Journal of Sound and Vibration* **117**, 467–474. In-plane vibrations of portal frames with end supports elastically restrained against rotation and translation.
6. C. H. Chang, P. Y. Wang and Y. W. Lin 1987 *Journal of Sound and Vibration* **117**, 233–248. Vibration of X-braced portal frames.
7. J. E. Mottershead, T. K. Tee and C. D. Foster 1990 *Journal of Vibration and Acoustics* **112**, 78–83. An experiment to identify the structural dynamics of a portal frame.
8. H. P. Lee and T. Y. Ng 1994 *Journal of Sound and Vibration* **172**, 420–427. In-plane vibration of planar frame structures.
9. R. W. Clough and J. Penzien 1975 *Dynamics of Structures*. New York: McGraw-Hill.
10. A. Alexandropoulos, G. Michaltsos and K. Kounadis 1986 *Journal of Sound and Vibration* **106**, 153–159. The effect of longitudinal motion and other parameters on the bending eigenfrequencies of a simple frame.

11. A. S. YIGIT 1994 *Journal of Sound and Vibration* **177**, 349–361. The effect of flexibility on the impact response of a two-link rigid-flexible manipulator.
12. J. L. JUNKINS and Y. KIM 1993 *Introduction to Dynamics and Control of Flexible Structures*. Washington, D.C.: AIAA. See pp. 116–175.
13. H. BANG 1996 *Journal of Guidance, Control and Dynamics* **19**(1), 248–250. Analytical solution for dynamic analysis of a flexible L-shaped structure.
14. A. D. DIMAROGONAS and S. HADDAD 1992 *Vibration for Engineers*. Englewood Cliffs, New Jersey: Prentice-Hall.

APPENDIX A: NOMENCLATURE

A_i	cross-sectional area of the ith beam
E_i	Young's modulus of the ith beam
I_i	second moment of the area of the ith beam
L	ratio of the length of the second beam to the first beam
L_i	length of the ith beam
m_t	mass of the tip mass
M_t	non-dimensional mass of the tip mass
$\mathbf{r}_i$	position vector of an elemental mass of the ith beam
t	time
T	system kinetic energy
U	system potential energy
$v_i(x_i, t)$	transverse displacement of the ith beam
$V_i(u_i)$	eigenfunctions of the ith beam
x_i	co-ordinate of the ith beam
α	slope at the end of the first beam
θ	orientation of the second beam relative to the first
λ_i	non-dimensional frequency of the ith beam
ξ_i	non-dimensional co-ordinate of the ith beam
ρ	ratio of the length density of the first beam to the length density of the second beam
ρ_i	volume mass density of the ith beam
ω	natural frequency
$\dot{()}$	time derivative
$()'$	spatial derivative

APPENDIX B: ELEMENTS OF MATRIX A

Using the notation that

$$S_\theta = \sin(\theta), \quad C_\theta = \cos(\theta), \quad s_1 = \sin(\lambda_1), \quad c_1 = \cos(\lambda_1),$$
$$sh_1 = \sinh(\lambda_1), \quad ch_1 = \cosh(\lambda_1), \quad s_2 = \sin(\lambda_2), \quad c_2 = \cos(\lambda_2),$$
$$sh_2 = \sinh(\lambda_2), \quad ch_2 = \cosh(\lambda_2),$$

the elements of the matrix, A_{ii}, are given as

$$A_{11} = \frac{1}{L} C_\theta (sh_1 - s_1), \quad A_{12} = \frac{1}{L} C_\theta (ch_1 - c_1), \quad A_{13} = 0, \quad A_{14} = 1,$$
$$A_{15} = 0, \quad A_{16} = 1, \quad A_{21} = \lambda_1 (ch_1 - c_1), \quad A_{22} = \lambda_1 (s_1 + sh_1),$$
$$A_{23} = \lambda_2, \quad A_{24} = 0, \quad A_{25} = \lambda_2, \quad A_{26} = 0,$$
$$A_{31} = 0, \quad A_{32} = 0, \quad A_{33} = -\lambda_2^2 s_2, \quad A_{34} = -\lambda_2^2 c_2,$$
$$A_{35} = \lambda_2^2 sh_2, \quad A_{36} = \lambda_2^2 ch_2, \quad A_{41} = 0, \quad A_{42} = 0,$$
$$A_{43} = \lambda_2^3(\lambda_2 M_t s_2 - \rho L c_2), \quad A_{44} = \lambda_2^3(\lambda_2 M_t c_2 + \rho L s_2),$$

$$A_{45} = \lambda_2^3(\lambda_2\, M_t\, sh_2 + \rho L ch_2), \qquad A_{46} = \lambda_2^3(\lambda_2\, M_t\, ch_2 + \rho L sh_2),$$

$$A_{51} = \lambda_1^2(s_1 + sh_1), \qquad A_{52} = \lambda_1^2(c_1 + ch_1),$$

$$A_{53} = \lambda_1^4 L^2\left(\rho L\left(\frac{s_2}{\lambda_2^2} - \frac{c_2}{\lambda_2}\right) + M_t\, s_2\right), \qquad A_{54} = \lambda_1^4 L^2\left(\rho L\left(\frac{c_2}{\lambda_2^2} + \frac{s_2}{\lambda_2} - \frac{1}{\lambda_2^2}\right) + M_t\, c_2\right),$$

$$A_{55} = \lambda_1^4 L^2\left(\rho L\left(\frac{ch_2}{\lambda_2} - \frac{sh_2}{\lambda_2^2}\right) + M_t\, sh_2\right), \qquad A_{56} = \lambda_1^4 L^2\left(\rho L\left(\frac{sh_2}{\lambda_2} - \frac{ch_2}{\lambda_2^2} + \frac{1}{\lambda_2^2}\right) + M_t\, ch_2\right),$$

$$A_{61} = -\lambda_1^3(c_1 + ch_1) + \lambda_1^4(\rho L + M_t)\,(s_1 - sh_1)S_\theta^2,$$

$$A_{62} = \lambda_1^3(s_1 - sh_1) + \lambda_1^4(\rho L + M_t)\,(c_1 - ch_1)S_\theta^2,$$

$$A_{63} = \lambda_1^4 L\left(\rho L\left(\frac{1}{\lambda_2} - \frac{c_2}{\lambda_2}\right) + M_t\, s_2\right)C_\theta, \qquad A_{64} = \lambda_1^4 L\left(\rho L\,\frac{s_2}{\lambda_2} + M_t\, c_2\right)C_\theta,$$

$$A_{65} = \lambda_1^4 L\left(\rho L\left(\frac{ch_2}{\lambda_2} - \frac{1}{\lambda_2}\right) + M_t\, sh_2\right)C_\theta, \qquad A_{66} = \lambda_1^4 L\left(\rho L\,\frac{sh_2}{\lambda_2} + M_t\, ch_2\right)C_\theta.$$